

## Accepted Manuscript

Techno-Economic Analysis of a Process for CO<sub>2</sub>-Free Coproduction of Iron and Hydrocarbon Chemical Products

B. Parkinson, C. Greig, E. McFarland, S. Smart

PII: S1385-8947(16)31807-1

DOI: <http://dx.doi.org/10.1016/j.cej.2016.12.059>

Reference: CEJ 16224

To appear in: *Chemical Engineering Journal*

Received Date: 4 September 2016

Revised Date: 23 November 2016

Accepted Date: 13 December 2016



Please cite this article as: B. Parkinson, C. Greig, E. McFarland, S. Smart, Techno-Economic Analysis of a Process for CO<sub>2</sub>-Free Coproduction of Iron and Hydrocarbon Chemical Products, *Chemical Engineering Journal* (2016), doi: <http://dx.doi.org/10.1016/j.cej.2016.12.059>

This is a PDF file of an unedited manuscript that has been accepted for publication. As a service to our customers we are providing this early version of the manuscript. The manuscript will undergo copyediting, typesetting, and review of the resulting proof before it is published in its final form. Please note that during the production process errors may be discovered which could affect the content, and all legal disclaimers that apply to the journal pertain.

# Techno-Economic Analysis of a Process for CO<sub>2</sub>-Free

## Coproduction of Iron and Hydrocarbon Chemical Products

Parkinson, B.<sup>a</sup>, Greig, C.<sup>a</sup>, McFarland, E.<sup>b</sup> & Smart, S.<sup>a,\*</sup>

<sup>a</sup> The University of Queensland, Dow Centre for Sustainable Engineering Innovation, School of Chemical Engineering, St Lucia, QLD, 4072, Australia

<sup>b</sup> Department of Chemical Engineering, University of California Santa Barbara, CA 93106-5080, USA

\*Corresponding Author: s.smart@uq.edu.au

### Abstract

The economics of an integrated iron and hydrocarbon process utilizing molten salt electrolysis to produce 1850 kilotonnes per annum (kta) of reduced iron and 500 kta of higher hydrocarbons is presented. Capital and operating cost models based on Aspen Plus V8.6 sizing data were used to generate cash-flow and production costs for the proposed scheme. The process economics are most strongly dependent on the natural gas and electricity prices. The capital cost estimates include high contingency costs to reflect the higher investment risk for a first-of-a-kind (FOAK) process. At a carbon price of less than US \$30/tCO<sub>2</sub>e, the process is competitive with traditional

### ABBREVIATIONS

EAF	Electric Arc Furnace
BF	Integrated Blast Furnace
BOF	Basic Oxygen Furnace
DRI	Direct Reduced Iron
CCS	Carbon Capture and Sequestration
OCM	Oxidative Coupling of Methane
IEA	International Energy Association
kta	Kilotonnes Per Annum
TEA	Techno-Economic Analysis
FOAK	First-of-a-kind
PCE	Purchased Cost of Equipment
FCI	Fixed Capital Investment
TCI	Total Capital Investment
OPEX	Operating Expenses
IRR	Internal Rate of Return
PRWS	Peng-Robinson Wong-Sandler
DC	Direct Costs
FC	Fixed Capital

blast furnace smelting. Areas where a more complete understanding is needed of the barriers to the deployment of this technology are identified.

**Keywords:** Low CO<sub>2</sub> Iron, Hydrocarbon conversion, Carbon price, Natural gas conversion, Iron electrolysis, Inorganic acid leaching

---

## 1. Introduction

Industrial manufacturing is a cornerstone of the global economy. It is a significant challenge for large producers of metals and chemicals to remain cost competitive whilst simultaneously lowering emissions and maintaining process energy and feedstock efficiency [1-2]. Manufacturing industries are responsible for approximately 30% of global CO<sub>2</sub> emissions and iron and steel production is the largest industrial source of direct CO<sub>2</sub> emissions estimated to be about 6-7% of the total global anthropogenic CO<sub>2</sub> [3].

The carbon intensity of different iron and steel production routes varies considerably, ranging from 0.4 tCO<sub>2</sub>/t crude steel for scrap/electric arc furnaces (EAFs), 1.7-1.8 tCO<sub>2</sub>/t crude steel for integrated blast furnace (BF) basic oxygen furnaces (BOFs) to 2.5 tCO<sub>2</sub>/t crude steel for coal-based direct reduced iron (DRI) processes [3]. Of these, the integrated BF-BOF route is the most widely used, accounting for approximately 70% of the world crude steel production in 2010 [4]. The majority of the emissions (~1.8 tCO<sub>2</sub> / t crude steel average) come from the high temperature reduction of iron ore which today occurs through the oxidation of carbon feedstocks (e.g. coke) [5].

The production of metallic iron requires the chemical reduction of ores. Replacing coke as a reducing agent for the oxide ores with less carbon intensive feedstocks including natural gas, hydrogen (sourced from fossil fuels), or biomass have been investigated [6-7]. However, these

methods have limited economic viability or unacceptable secondary environmental consequences and in some cases simply pass the emissions upstream [8].

Significant reduction in CO<sub>2</sub> emissions (>50% of current emissions) is achievable through carbon capture and storage (CCS) [9]. The deployment of CCS technologies within an integrated steel mill is technically feasible and has been the subject of significant research [7, 9-11]. Indeed, CCS represents the largest portion of emissions reductions in the International Energy Association (IEA) emission reduction roadmaps for the iron and steel industry [1]. The complexities of integration, the high cost and energy penalty associated with capture from relatively dilute flue gas streams and the uncertainties of geological sequestration, mean that CO<sub>2</sub> avoidance costs for 50% emissions reductions and higher have been estimated in excess of US \$74/tCO<sub>2</sub> avoided for current best available technologies [9].

An alternative is to electrochemically reduce the iron oxide as is done for other metal oxide ores. This is not currently economically feasible due to the high temperatures (>1500°C) required for iron ore reduction [12]. Chemical upgrading of iron ore through leaching to facilitate low temperature electrolysis of iron has also been investigated but prohibitively high processing costs have inhibited its development in industry [13-14].

Olefins such as ethylene and propylene represent the largest volume of organic chemicals produced globally. In contrast to iron produced by reduction of oxide ores, the production of olefins requires partial oxidation of hydrocarbon carbon feedstocks. The most common processes require heating alkanes to very high temperatures and 'cracking' them in the presence of steam. Additional chemistry allows the production of a variety of important commodity chemicals including alcohols, aromatics, and a diverse range of high value hydrocarbons [15]. Natural gas and methane hydrates are likely to provide abundant low cost light alkanes as feedstocks for organic

chemicals for decades [16-17]. The CO<sub>2</sub> emissions result from the large quantities of energy required for modern olefin processing. Several hundred million tonnes of CO<sub>2</sub> each year are released to produce olefins [16]. Hydrocarbon processing and the chemical industry as a whole account for 17% of industrial CO<sub>2</sub> emissions (5.5% global CO<sub>2</sub> emissions) [2].

Efforts to use light alkanes to produce olefins and aromatics by selective partial oxidation and oxidative coupling of methane (OCM) using limited oxygen have been ongoing [18]. These catalytic processes have been identified as providing the largest potential for greenhouse gas emissions reductions in the IEA chemical industry roadmaps [2]. Despite decades of investigation, fundamental chemical limitations and practical challenges in catalysis remain and there is no evidence an economically competitive process is possible [19-23]. It has not been possible to demonstrate sustained high reaction rates of oxygen with light alkanes without producing large quantities of carbon oxides.

Partial oxidation of methane and other light alkanes using alternative oxidants such as halogens has been demonstrated and operated in pilot plants [24-26]. Reactions of halogens including chlorine and bromine with methane or other light alkanes generate alkyl-halide intermediates which are readily transformed into olefins and aromatic products. The process technology is an alternative to the conventional steam cracking and dehydrogenation processes. For methane, the methyl-halide intermediate undergoes the same types of chemical transformations as methanol to form olefins (methanol-to-olefins [27]) or aromatics (methanol-to-aromatics [28]). The main challenges to widespread commercialization of the halogen-based processes are the costs of recycling stoichiometric quantities of corrosive hydrogen halides which are used to regenerate the halogen and the thermal management of the exothermic reactions [29-30].

We propose a unique process that couples the reduction of iron ore with the partial oxidation of natural gas alkanes to co-produce iron and organic chemicals. Iron ore is upgraded by reaction with hydrogen chloride and the iron chlorides electro-reduced to the iron product. The oxidized iron chlorides are used for reaction with methane to produce the methyl-chloride intermediates. These are subsequently converted to hydrocarbon chemical products and the hydrogen chloride reused. No CO<sub>2</sub> is produced. The integrated process overcomes the limitations of the conventional iron ore electrolysis and methane partial oxidation processes using halogens through:

- Substitution of the pure halogen for a liquid metal halide (FeCl<sub>3</sub>) as the oxidising agent to advantageously manage the exothermic heat load;
- Leaching iron ore with the inorganic acid (HCl) generated as a by-product to create a higher-value iron feedstock to an electrolyser (eliminating the major feedstock cost for leaching on the iron side);
- Regeneration of the iron chloride feedstock via the production of reduced iron from electrolysis (eliminating the major regeneration cost of the halogen).

It is generally expected that a price will be placed on atmospheric carbon emissions at some time [31]. This will significantly impact both the iron and chemical industries and may have far reaching economic consequences for infrastructure, construction, transport, advanced manufacturing and consumer products [19]. In this paper we examine the techno-economics of a production process that co-produces iron and hydrocarbon products and makes use of process integration and process intensification for overall efficiency and economic gains. Specifically, we address the following questions: What are the estimated capital and operating costs of the integrated process? What are the sensitivities of the costs to the major process uncertainties? What cost of carbon dioxide (CO<sub>2</sub> price) would be needed for such a process to be economically competitive with present commercial processes?

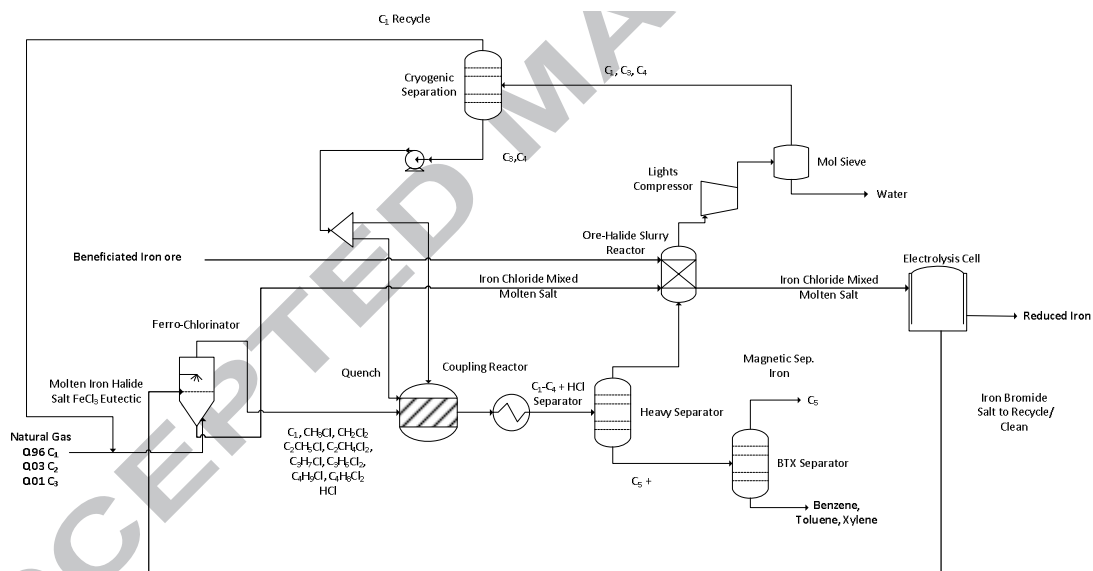
### 1.1 Process Description

A simplified process flow diagram of the proposed coupled process is shown in Figure 1. Methane from pre-treated natural gas is supplied to the ferro-chlorination reactor, where the facile reaction of methane with molten ferric chloride to produce ferrous chloride, hydrogen chloride and methyl chloride occurs (Equation 1). Chlorination of methane using redox active chlorinated molten salts is expected to reduce the exothermic heat load of the chlorination reaction due to the endothermic  $\text{Cl}^-$  evolution reaction [32]. The relatively small heat load is managed through absorption into a high thermal capacity molten salt. The methyl chloride product is coupled over zeolite catalysts to higher saturated and unsaturated hydrocarbons and aromatics (Equation 2). The hydrogen chloride by-product is used to leach the beneficiated iron ore feedstock, converting the insoluble oxide to soluble chlorides ( $\text{FeCl}_2/\text{FeCl}_3$ ) and water (Equation 3), creating a higher value feedstock for electrolysis. The mixed ferric/ferrous soluble metal chloride feed undergoes molten electrolysis according to Equation 4 (Equations 4.1 and 4.2 half cells), regenerating the metallic halide feedstock. Essentially, the regenerable molten halide salt-based chemical cycle is used in the first instance, to simplify gas-to-liquid processes through an alternative method for regeneration of the halogen, and to produce reduced iron without  $\text{CO}_2$ .

Table 1: Simplified system of equations in the Dow Centre Process

Equation	No.
$\text{CH}_4 + 2 \text{FeCl}_3 \rightarrow 2 \text{FeCl}_2 + \text{CH}_3\text{Cl} + \text{HCl}$	1
$n\text{CH}_3\text{Cl} \rightarrow (\text{CH}_2)_n + n\text{HCl}$	2
$1/2 \text{Fe}_3\text{O}_4 + 4 \text{HCl} \leftrightarrow 1/2 \text{FeCl}_2 + \text{FeCl}_3 + 2\text{H}_2\text{O}$	3
$4.5 \text{FeCl}_2 \rightarrow 3 \text{FeCl}_3 + 1.5 \text{Fe}^0$	4
$\text{FeCl}_2 + 2 e^- \leftrightarrow \text{Fe} + 2 \text{Cl}^-$	4.1
$2 \text{FeCl}_2 + 2 \text{Cl}^- \leftrightarrow 2 \text{FeCl}_3 + 2 e^-$	4.2

Figure 1: Simplified process flow diagram of an integrated iron/petrochemicals co-production process plant.



Whilst the individual reactions presented in Table 1 have been the subject of investigation by others (halogenation of methane using metal chlorides [30, 33-34], more specifically ferric chloride [35], coupling of methyl halides [25, 36-38], leaching of iron ore with HCl [39-41], iron-chloride redox flow batteries [42-43]), in this report we present a unique process intensification which couples each of these individual concepts.



## 2. Process Economics

The design basis for the process is iron production of 1850 kilotonnes per annum (kta) from 2690 kta of beneficiated iron ore ( $\text{Fe}_3\text{O}_4$ ) and co-processing of 575 kta of natural gas. The techno-economic analysis (TEA) reported here incorporates capital cost estimates with relatively high contingency factors, reflecting a higher risk investment for a first-of-a-kind (FOAK) facility [44]. A construction period of three years and 12-month start-up period operating at 50% of name-plate capacity has been used.

An ASPEN Plus conceptual process model was developed to obtain equipment sizing and costing data for calculating the purchased cost of equipment (PCE). For some major pieces of equipment, additional correlations and/or discussions with original equipment manufacturers were used to reduce cost uncertainty. Fixed and total capital investments (FCI and TCI, respectively) were developed through well-established factorial methods [45].

The natural gas pre-treatment (i.e. hydrodesulphurization) was not modelled, however, the cost of pipeline natural gas is included in the analysis. Based on the mass and energy balances, other fixed and variable non-capital estimates were made of the operating expenses (OPEX). With total operating and capital costs determined, a discounted cash flow analysis was performed to determine key investment indicators. A summary of the assumptions and financial inputs is provided in Table 2.

For comparison purposes, different  $\text{CO}_2$  prices are used to calculate the required price ( $\$/\text{tCO}_2$  emitted) needed to raise the internal rate of return (IRR) for the investment to above 10% (nominal, after tax). This is calculated by assuming full pass-through of the carbon price, i.e. by increasing the product value of iron produced by conventional blast furnace technology ( $1.8 \text{ tCO}_2/\text{t}$  iron) by the full carbon price. This assumption is justified for low to moderate carbon prices as no

alternative processes are economically competitive, for example iron making with integrated CCS has an estimated minimum carbon price of US \$74/tCO<sub>2</sub> [9].

Table 2: Assumptions for FOAK Process TEA

<b>Economic Parameters</b>	
<b>Year of Analysis</b>	2016
<b>Construction Period</b>	3 Years
<b>Start-up Period</b>	12 months
<b>Start-up Capacity</b>	50%
<b>Plant Lifetime</b>	25 years
<b>On-Stream Factor</b>	91%
<b>Inflation</b>	2%
<b>Weighted Average Cost of Capital (WACC)</b>	10% (Nominal, After Tax)
<b>Depreciation</b>	Straight Line
<b>Depreciation Period</b>	10 Years
<b>Company Tax Rate</b>	35%
<b>Location</b>	U.S. Gulf Coast

To effectively compare direct and indirect CO<sub>2</sub> emissions from each process, the carbon intensity of electricity supplied has been assumed to be supplied from a combined cycle gas turbine operating according to U.S. Environmental Protection Agency Clean Power Plan, releasing approximately 0.467 tCO<sub>2</sub>/MWh supplied [46]. This level of electricity carbon intensity is considered conservative for a transition scenario where power is predominately supplied by a mixture of nuclear, gas and renewable technologies and is investigated further in a sensitivity analysis.

### 3. Methods - Conceptual Process Modelling

The conceptual process model developed in ASPEN Plus V8.6 is used to simulate the integration of the molten halide salt loop with a methane gas-to-liquid hydrocarbon product process. The Peng-Robinson Wong-Sandler (PRWS) thermodynamic property method was selected to model the hydrocarbon processing as this package is suitable for mixtures of non-polar and polar components in light gases above 10 bar operating pressure [47]. However, due to the lack of kinetic data available for methane molten iron chloride reactions, the ferro-chlorinator reactor was sized based on the kinetic data of the chlorination of methane with copper chloride melts reported by Fontana et al [32]. Whilst this represents a gap in existing knowledge, it is expected that natural gas chlorination via ferric chloride will exhibit similar kinetics to other redox active metal chloride mixed chloride salt systems.

In the ferro-chlorination reactor, pre-treated natural gas (molar feed composition 96% CH<sub>4</sub>, 3% C<sub>2</sub>H<sub>6</sub>, 1% C<sub>3</sub>H<sub>8</sub>) is fed in a stoichiometric ratio with ferric chloride of 1:2, reacting according to the overall system of equations shown in Table 3. The ferric chloride is diluted in a 50% NaCl salt solution for two purposes: minimising volatility of ferric chloride up to 600°C and to lower the eutectic melting point of ferrous chloride product to below 400°C [48-49]. The natural gas feedstock is oxidised at 28 bar and 400°C via the molten halide salt. The design basis is a single pass methane conversion of 80%, and 100% conversion of the small fractions of ethane and propane in the feed gas [38]. The single pass methane conversion of 80% has been assumed achievable based on halogenation work from Lorkovic et al [38] who achieved gas phase methane conversions with bromine of 70-75% in a single pass. The proportion of poly-alkylchlorides is easily managed in the coupling reactor [50], the mono:di chlorination ratio is fixed at 90:10 for the purposes of this analysis.

Table 3: Overall reaction mechanisms of the halogenation reactor

Reaction at 450 °C	Equ. No.	$\Delta H$ (kJ/mol)
$\text{CH}_4 + 2 \text{FeCl}_3 \rightarrow 2 \text{FeCl}_2 + \text{CH}_3\text{Cl} + \text{HCl}$	(2)	-88
$2 \text{FeCl}_3 + \text{CH}_3\text{Cl} \rightarrow \text{CH}_2\text{Cl}_2 + 2 \text{FeCl}_2 + \text{HCl}$	(5)	-90
$\text{C}_2\text{H}_6 + 2 \text{FeCl}_3 \rightarrow 2 \text{FeCl}_2 + \text{C}_2\text{H}_5\text{Cl} + \text{HCl}$	(6)	-106
$\text{C}_2\text{H}_5\text{Cl} + 2 \text{FeCl}_3 \rightarrow 2 \text{FeCl}_2 + \text{C}_2\text{H}_4\text{Cl}_2 + \text{HCl}$	(7)	-94
$\text{C}_3\text{H}_8 + 2 \text{FeCl}_3 \rightarrow 2 \text{FeCl}_2 + \text{C}_3\text{H}_7\text{Cl} + \text{HCl}$	(8)	-102
$\text{C}_3\text{H}_7\text{Cl} + 2 \text{FeCl}_3 \rightarrow 2 \text{FeCl}_2 + \text{C}_3\text{H}_6\text{Cl}_2 + \text{HCl}$	(9)	-93

The ferro-chlorinator reactors operate as 4 trains of counter-current gas flow through bubbling reactor columns, with maximum void fractions from gas holdup <0.3 [51]. The sizing parameters of the ferro-chlorinator are summarized in Table 4.

Table 4: Ferro-chlorinator reactor design parameters

Component	Factor
Reactors in Parallel	4
Bubble Rise Velocity	0.3 m/s
Gas Residence Time	35 s
Excess Reactor Volume	20 %
Reactor Diameter	6.3 m
Reactor Height	11 m
Total Volume	340 m <sup>3</sup>

The alkyl-chloride coupling reactor assumes 100% conversion of the alkyl-chlorides to heavier hydrocarbons (alkanes, alkenes and aromatics) with the same selectivity demonstrated by Lorkovic et al [25]. The reproporation section of the reactor converts poly-chlorinated hydrocarbons to mono-chlorinated hydrocarbons through reactions with recycled alkanes and alkenes ( $C_3$ 's and  $C_4$ 's) according to the reaction scheme proposed by Pitt et al and Gadewar et al over zeolite catalysts [47, 52]. The reproporation of  $C_1$ - $C_5$  alkanes with dichloromethane occurs at similar temperatures to the coupling reaction [37]. Achieving higher initial methane conversion in the halogenation reactor increases the proportion of poly-halogenated hydrocarbons requiring reproporation. Increasing the proportion of mono-halogenated species present in the coupling reaction feed promotes the formation of higher molecular weight hydrocarbons and reduces catalyst deactivation via coking.

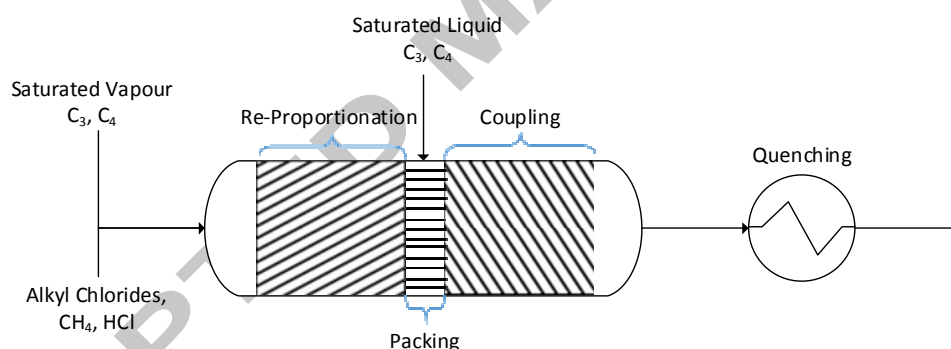


Figure 2: Schematic representation of the design of the coupling reactor and subsequent product

The reproporation reaction is expected to proceed quite slowly at low pressures [38], but is accelerated at the feed pressure of 26 bar over a zeolite catalyst [37] to achieve a conservative residence time of 20 seconds [29]. The exothermic reproporation reaction is quenched through feeding a portion of the saturated alkane liquid from the recycled  $C_3$  and  $C_4$  alkanes to the mixed HCl and alkyl chloride stream at approximately 400°C.

The exothermic heat load of the coupling reactions is managed through injecting the remaining saturated alkane liquid to a ceramic packed section of the reactor. The ceramic packing facilitates the alkane vaporization and prevents back mixing, quenching the feed to the coupling section of the reactor design. The coupling reaction over a ZMS-5 catalyst at approximately 450°C-500°C is very fast, going to completion in approximately 5 seconds [26]. To process the volumetric gas flow, two reactors are required operating in parallel, with a 3<sup>rd</sup> reactor available to cycle for coke removal. The sizing dimensions of the coupling reactor are summarized in Table 5.

Table 5: Coupling Reactor design parameters

Component	Factor
Reactors in Parallel	3
Reproportionation	20 s
<b>Residence Time</b>	
Coupling Residence Time	5 s
Reactor Diameter	2.8 m
Reactor Length	22.5 m
Catalyst Loading	30%

The HCl and the mixture of hydrocarbons are quickly quenched after coupling to circumvent re-addition of HCl across alkene bonds [29]. Higher hydrocarbons (C5<sup>+</sup>) are separated using a RadFrac simulation capable of modelling multistage vapour/liquid fractionation operations and further processed for product purity requirements. The light hydrocarbons and HCl are sent to the ore-halide slurry reactor, where HCl is completely reacted with the sparingly soluble iron oxide suspended in molten chloride, converting the oxide to soluble chlorides via reaction 4 and the hydrocarbon mixture passes through in the gas phase with minimal cracking [29]. This unique process design avoids costly cryogenic separation of large volumes of HCl from lower alkanes.

Further downstream separation of the hydrocarbon mixture from water generated in reaction 4 occurs prior to recycling the unconverted lower alkanes.

The ore-halide slurry reactor is sized with the same methodology as the ferro-chlorination reactor. The high solubility of HCl in molten chloride salts [53-54] facilitates effective contact for reduction of  $\text{Fe}_3\text{O}_4$ . The reduction of  $\text{Fe}_3\text{O}_4$  with hydrogen halides (chlorine and bromine) has been the subject of investigation by many interested in thermochemical cycles for  $\text{H}_2$  production [39-41, 55]. The reduction reaction of  $\text{Fe}_3\text{O}_4$  with HCl is known to proceed rapidly, with the reaction products very strongly depending upon experimental conditions. Gas phase formation of the  $\text{Fe}_2\text{Cl}_6$  (g) dimer above the boiling point of  $\text{FeCl}_3$  is suppressed due to the low vapour pressure of molten NaCl salts and the common ion effect [48].

The impact of iron ore impurities such as carbon, sulphur and phosphorus on the product distribution is known to cause a favourable shift to  $\text{FeCl}_2$  production [39], but the extent of this impact on the overall system design is unknown and is the subject of further investigation. The dissolution of magnetite in concentrated acid solutions has been studied much less compared to other iron oxides, but is known to proceed at faster rates due to catalysis of the lattice dissolution by containing both Fe(II) and Fe(III) [56]. For the ore-halide slurry reactor, 4 reactors are proposed in parallel and the sizing dimensions of the coupling reactor are summarized in Table 6.

Table 6: Ore-Halide Slurry Reactor design parameters

Component	Factor
Reactors in Parallel	4
Bubble Rise Velocity	0.3 m/s
Gas Residence Time	41 s
Excess Reactor Volume	20 %

<b>Reactor Diameter</b>	7.2 m
<b>Reactor Height</b>	12.3 m
<b>Total Volume</b>	450 m <sup>3</sup>
<b>Material</b>	CS + HS Lining

The molten iron chloride salt leaving the ore-halide slurry reactor is sent to an iron-chloride redox electrolyser, which operates according to Figure 3 [42]. The redox chemistry is based on the iron (II) chloride/iron (III) chloride redox couple at the positive electrode and the iron (II) chloride/metallic iron couple at the negative electrode [42]. The open-circuit voltage is 1.21 V; however, an overpotential must be expected to drive acceptable current densities. There is insufficient information to quantitatively assess the impact of overpotential, parasitic losses and the potential production of by-products (e.g. Cl<sub>2</sub> at the anode or H<sub>2</sub> at the cathode) on the cost and complexity of the electrolyser and we have excluded them from the model. The 'all-iron' redox flow battery has been the subject of much interest in the field of large-scale energy storage systems since its conceptualization by Hruska and Savinell in 1981 [57]. Many of the technical and process challenges of the all-iron battery have since been well defined and significant technological and commercialization progress has been made [42, 58] and is not explored further here.

In this process, many of the current cycling and performance life issues associated with redox flow battery are avoided due to employing the concept uni-directionally, not requiring the discharge step of redox flow battery process. Simply put, the iron plated on the iron electrode is removed and the ferric chloride regenerated at the positive electrode is recycled to the halogenation reactor at the beginning of the process to oxidise the natural gas feedstock. A schematic of a traditional iron-chloride flow battery is shown in Figure 3.



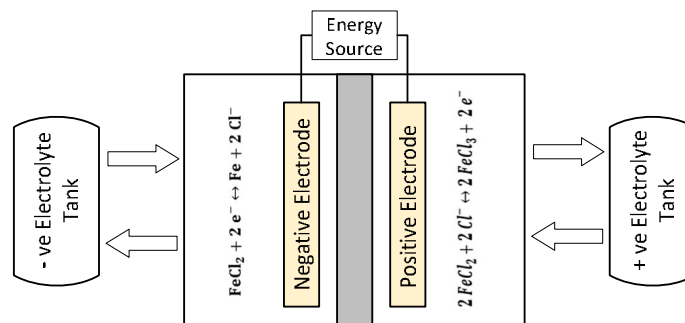


Figure 3: Schematic of the principle of operation of an iron-chloride redox flow battery [42, 58].

Design considerations included the materials of construction required to handle corrosive molten salts and hydrochloric acid. Any material in contact with hydrochloric acid or the molten ferroschlorinated salt is lined with hastelloy C (HS) to minimise corrosive attack. For all other materials of construction unless otherwise specified, carbon steel (CS) has been used as it possessed sufficient material properties to handle hydrocarbons. The materials are summarized in Table 7.

Table 7: Materials of Construction for corresponding unit operations.

Name	Material
Chlorination Reactor	CS + HS
Coupling Reactor	CS + HS
Quench Exchanger	CS (Shell) + HS (Tube)
Heavy Separator	CS + HS
BTX Separator	CS
Ore-Halide Slurry Reactor	CS + HS
Electrolyser	CS + HS

Mol Sieve	CS
Lights Compressor	CS
Cryogenic Separation	SS
Salt Pump	HS
Salt Cooler	CS (S) + HS (T)
Flash Tank	CS

#### 4. Results and Discussion

Steady-state process simulation results based on an 80% single pass conversion of methane in the ferro-chlorination reactor, 100% conversion of alkyl chlorides in the coupling reactor and 100% neutralization of HCl in the ore-halide slurry reactor are summarized in Table 8. The electrolyser electricity consumption accounts for approximately 87% (320 MW) of the total process power consumption (367 MW).

Table 8: Model Production Summaries

Product	Quantity
Reduced Iron	1850 KTA
C <sub>5</sub> Pentane	150 KTA
C <sub>5</sub> Pentene	19 KTA
Benzene	68 KTA

Toluene	136 KTA
Xylene	127 KTA

The process variables found to have significant impact on the process performance and cost include; reactant compositions, conditions, and reaction rates which have a major effect on the design and sizing of vessels and downstream separation processes. For example, hydrochloric acid in the presence of water significantly influences the cost of the materials required to limit corrosion in the process units. Allowances are made to account for these added costs where halogens are present.

The estimated total purchased cost of equipment for the current process design is \$160.5 million USD. A breakdown of the costs determined using the ASPEN Icarus software package and, for the electrolyser, costs from actual costs of installed electrolysers scaled on current density, is shown in Figure 4. It is apparent the most expensive unit costs are the hastelloy lined reactor vessels, totalling 49% of the PCE. These costs might be reduced through improving selectivity to higher hydrocarbons or more accurate kinetics to support reducing the reactor residence times. The project TCI is estimated to be \$1927 million including working capital and start-up costs. The factors used to calculate the TCI from the PCE along with the other principal cost parameters are summarized in

Table 9. For a FOAK process with engineering definition still conceptual only, a Lang Factor of 10 applied to the purchased equipment costs [59]. This effectively applies a contingency cost of 180% to direct capital costs. The total OPEX is summarised in

Table 10, based on the current design the total OPEX is \$284.2 million USD/yr. The operating costs are dominated by the electricity charge of supplying approximately 320 MW to the electrolyser, accounting for 59% of the total OPEX.

Figure 4: Breakdown of purchased cost of equipment costs

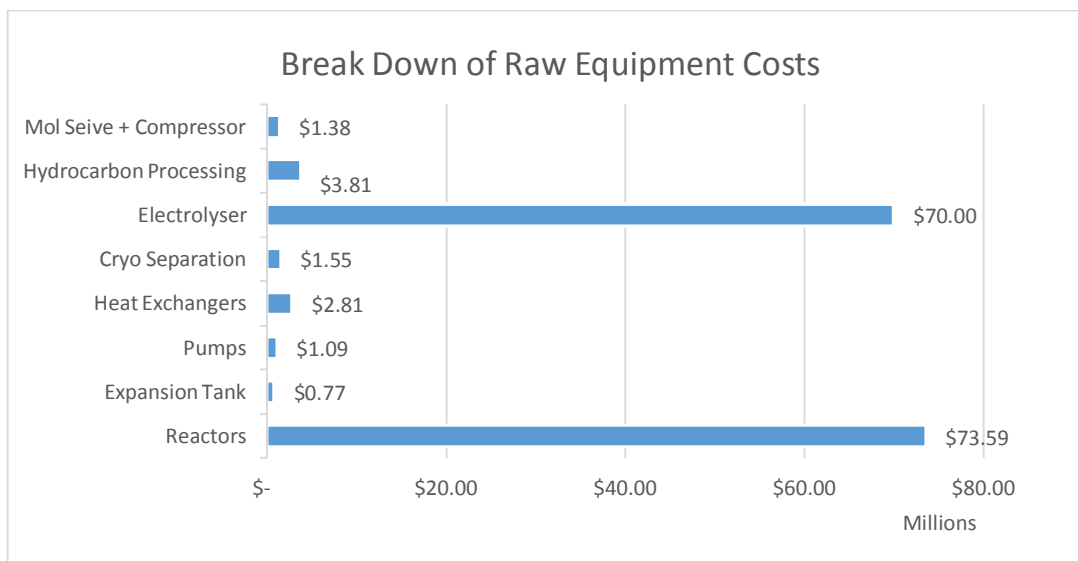


Table 9: Total Capital Investment Cost Breakdown

Parameter	Cost (\$US, Millions)
<b>Purchased Equipment</b>	\$160.5
<b>Cost</b>	
<b>Equipment installation</b>	40% PCE
<b>cost</b>	
<b>Piping</b>	60% PCE Non-Halogen

	80% Halogen
<b>Instrumentation</b>	20% PCE
<b>Electrical</b>	10% PCE
ISBL	<b>\$384</b>
<b>Buildings</b>	15% PCE
<b>Site improvement</b>	5% PCE
<b>Utilities</b>	40% PCE
<b>Storage</b>	15% PCE
<b>Auxiliary facilities</b>	15% PCE
OSBL	<b>\$160.5</b>
<b>Direct costs (DC)</b>	<b>\$544.7</b>
<b>EPC</b>	15% of DC
<b>Contingency</b>	180% DC
Indirect costs	<b>\$1,061</b>
<b>Lang Factor</b>	10
Fixed capital (FC)	<b>\$1,606</b>
<b>Working capital</b>	10% of FC
<b>Start-up costs</b>	10% of FC
Total capital investment	<b>\$1,927</b>

Table 10: Operating Costs

<b>Cost Item</b>	<b>Basis</b>	<b>\$US, Millions/yr</b>
<b>Maintenance</b>	5% FC	45.2
<b>Labour</b>	200 Employees	20

<b>Operating</b>	10%	4.5
<b>Supplies</b>	Maintenance	
<b>Insurance</b>	4% FC	36.2
<b>Overhead</b>	50% Labour	10
<b>Electricity</b>	Calculated	168.3
<b>Total OPEX</b>		284.2

#### 4.1 Cash Flow and Sensitivity Analysis

For the discounted cash flow analysis, product values of \$250/t for reduced iron [60] and a conservative average value of \$700/t [61-62] for the hydrocarbons produced are used. Raw material costs of \$60/t for iron ore [60], \$4/GJ for natural gas [63] and \$0.06/kWh [64] for electricity are used. This generates annual revenues of \$813.8 million and an IRR of 5.4% with no carbon price in place. To achieve an IRR of 10%, a minimum carbon price of \$27/tCO<sub>2</sub> emitted is required. This value is sensitive to the model assumptions and raw material costs. The sensitivity of the economic analysis to the major factors affecting the viability of the process are illustrated as a tornado plot in Figure 5. Sensitivity bounds have been selected based on recent historic costs of inputs and outputs.

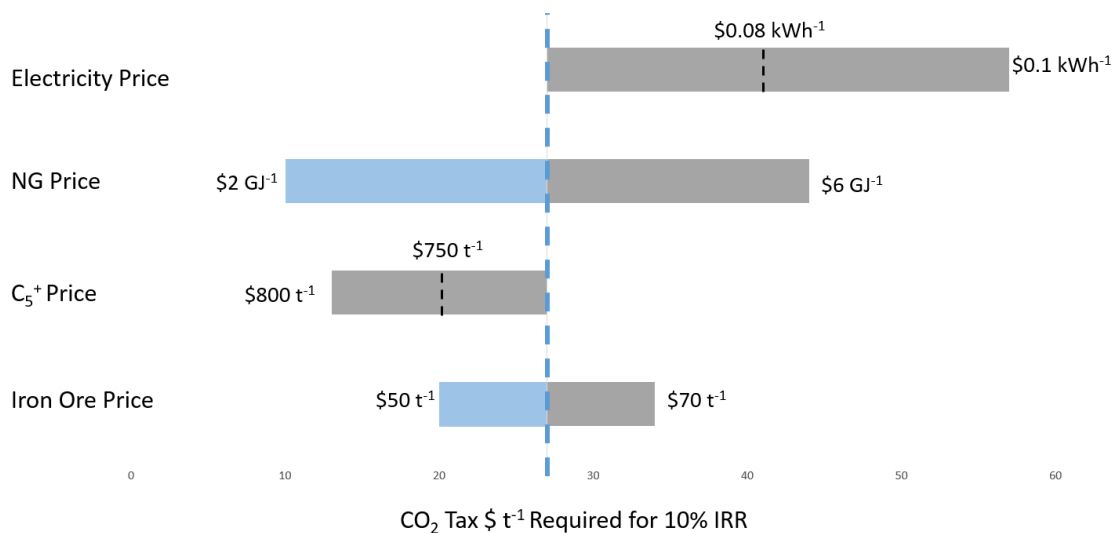


Figure 5: Sensitivity analysis of the major input variables to the CO<sub>2</sub> price required to achieve a 10% IRR.

The process economics are most sensitive to the electricity and natural gas costs which will be strongly dependent on the facility's location. The competitiveness of this new process compared with applying CCS to current blast furnace technologies will ultimately depend on the availability of competitively priced electricity and natural gas versus the availability of geological storage reservoirs and the cost of carbon capture technologies. Electricity from carbon-free nuclear power or renewable technologies further improves the carbon intensity and reduces the exposure to a price on carbon emissions. Even when very conservative contingency factors for a FOAK are used, the process shows economic promise even at relatively low imposed carbon prices for the current and the predicted future prices [16]. Under the influence of uncertain future market conditions and the adaptability of the existing chemistry and technology, this process integrating molten iron electrolysis with organic chemical production has the potential to compete with conventional iron production.

## 5. Summary and Future Work

Presently proposed pathways for transitioning to a carbon constrained future demand a price on carbon [31]. The production of iron without CO<sub>2</sub> through chemically upgrading the oxide ore for electrolysis using a by-product of hydrocarbon partial oxidation in this integrated process can reduce not only the environmental consequences of traditional manufacturing techniques, but minimise the far reaching economic impacts of carbon prices [19]. The process integration described here potentially eliminates major process costs for both processes, improving overall efficiency and process profitability. The use of methane from natural gas or other fossil hydrocarbons (i.e. propane) in this integrated process contributes to longer term use of low-cost hydrocarbon resources without CO<sub>2</sub> production. The process economics are highly dependent upon the availability of low cost hydrocarbon resources and electricity supplies. High contingencies have been allowed in the capital cost estimates and the process economics are still competitive with low imposed carbon prices.

Demonstrating the technical feasibility and improving the economic estimates to advance this proposed process is the subject of further work to verify the model assumptions. The ongoing work includes laboratory investigations of the:

- Rate of chlorination of ferric chloride-sodium chloride eutectic molten salt mixtures;
- Impact of impurities contained within beneficiated iron ore (i.e. carbon, sulphur, phosphorus) on overall reaction products and rate of iron ore reduction; and
- Purity of reduced iron product when electrolysed to an iron anode under system conditions.

#### ACKNOWLEDGEMENTS

This research did not receive any specific grant from funding agencies in the public, commercial, or not-for-profit sectors. The Authors acknowledge Mr Phil Grosso and Dr Howard Fong for their



invaluable advice in process design.

ACCEPTED MANUSCRIPT

## REFERENCES

- [1] International Energy Agency, "Technology Roadmap: Carbon Capture and Storage in Industrial Applications," International Energy Agency, 2011.
- [2] International Energy Agency, "Technology Roadmap: Energy and GHG Reductions in the Chemical Industry via Catalytic Processes," International Energy Agency, 2013.
- [3] A. Carpenter, "CO<sub>2</sub> abatement in the iron and steel industry," IEA Clean Coal Centre, 2012.
- [4] EPA, "Economic Impact Analysis of Final Iron and Steel Foundries NESHAP," Research Triangle Institute, North Carolina, 2003.
- [5] J.-P. Birat and J.-P. Vizoz, "CO<sub>2</sub> emissions and the steel industry's available responses to the greenhouse effect," in *Abatement of Greenhouse Gas Emissions in the Metallurgical & Materials Process Industry*, San Diego, 1999.
- [6] C. C. Amorim, P. R. Dutra, M. M. Leao, M. C. Perieira, A. B. Henriques, J. D. Fabris and R. M. Lago, "Controlled reduction of steel waste to produce active iron phases for environmental applications," *Chem. Eng. J. (Amsterdam, Neth.)*, vol. 209, pp. 645-651, 2012.
- [7] F. Ghanbari, F. Pettersson and H. Saxen, "Optimal operation strategy and gas utilization in a future integrated steel plant," *Chem. Eng. Res. Des.*, vol. 2, pp. 322-336, 2015.
- [8] L. J. Sonter, D. J. Barrett, C. J. Moran and B. S. Soares-Filho, "Carbon emissions due to the deforestation for the production charcoal used in Brazil's steel industry," *Nat. Clim. Change*, vol. 5, pp. 359-363, 2015.
- [9] IEAGHG, "Iron and Steel CCS Study (Techno-economics integrated steel mill)," IEAGHG, 2014.
- [10] L. Hooey, A. Tobiesen, J. Johns and S. Santos, "Techno-economic study of an integrated steelworks equipped with oxygen blast furnace and CO<sub>2</sub> capture," in *11th International Conference on Greenhouse Gas Technologies*, Kyoto, 2013.
- [11] D. Leeson, J. Fairclough, C. Petit and P. Fennell, "A systematic review of current technology and

- cost for industrial carbon capture," Grantham Institute, Imperial College, London, 2014.
- [12] A. Allanore, L. Yin and D. R. Sadoway, "A new anode material for oxygen evolution in molten oxide electrolysis," *Nat.*, vol. 497, pp. 353-356, 2013.
- [13] E. Mostad and S. T. J. Rolseth, "Electrowinning of iron from sulphate solutions," *Hydrometallurgy*, vol. 90, pp. 213-220, 2008.
- [14] M. Fishedick, J. Marzinkowski, P. Winzer and M. Weigel, "Techno-economic evaluation of innovative steel production technologies," *J. of clean. production*, vol. 84, pp. 563-580, 2014.
- [15] P. Perez-Uriarte, A. A. A. T. Ateka, A. G. Gayubo and J. Bilbao, "Kinetic model for the reaction of DME to olefins over a HZSM-5 zeolite catalyst," *Chem. Eng. J. (Amsterdam, Neth.)*, vol. 302, pp. 801-810, 2016.
- [16] IEA, "World Energy Outlook," International Energy Agency, 2015.
- [17] V. Arutyunov, V. Savchenko, I. Sedov, I. Fokin, A. Nikitin and L. Strekova, "New concept for small-scale GTL," *Chem. Eng. J. (Amsterdam, Neth.)*, vol. 282, pp. 206-212, 2015.
- [18] V. Mysov, S. Reshetnikov, V. Stepanov and K. Ione, "Synthesis gas conversion into hydrocarbons (gasoline range) over bifunctional zeolite-containing catalyst: experimental study and mathematical modelling," *Chem. Eng. J. (Amsterdam, Neth.)*, vol. 107, pp. 63-71, 2005.
- [19] J. Lunsford, "The catalytic conversion of methane to higher hydrocarbons," *Catal. Today*, vol. 6, no. 3, pp. 235-259, 1990.
- [20] J. J. Spivey and G. Hutchings, "Catalytic aromatization of methane," *Chem. Soc. Rev.*, vol. 43, no. 792, pp. 792-803, 2014.
- [21] T. Fini, C. Patz and R. Wentzel, "Oxidative coupling of methane to ethylene," University of Pennsylvania, Pennsylvania, 2014.
- [22] L. Luo, X. Tang, W. Wang, Y. Wang, S. Sun, Q. Fei and W. Huang, "Methyl radicals in oxidative

coupling of methane directly confirmed by synchrotron VUV photoionization mass spectroscopy," *Nature*, 2013.

- [23] A. Agiral, T. Nozaki, M. Nakase, S. Yuzawa, K. Okazaki and J. Gardeniers, "Gas-to-liquids process using multi-phase flow, non-thermal plasma microreactor," *Chem. Eng. J. (Amsterdam, Neth.)*, vol. 167, no. 2-3, pp. 560-566, 2011.
- [24] X.-P. Zhou, A. Yilmaz, G. A. Yilmaz and P. C. Ford, "An Integrated process for partial oxidation of alkanes," *Chem. Commun.*, vol. 18, pp. 2294-2295, 2003.
- [25] I. M. Lorkovic, A. Yilmaz, G. A. Yilmaz, X.-P. Zhou, L. E. Laverman, S. Sun, D. J. Schaefer, M. Weiss, M. L. Noy, I. C. Cutler, J. H. Sherman, E. W. McFarland, G. D. Stucky and P. C. Ford, "A novel integrated process for the functionalization of methane and ethane: bromine as mediator," *Catal. Today*, vol. 98, no. 1-2, pp. 317-322, 2004.
- [26] I. M. Lorkovic, M. L. Noy, W. A. Schenck, M. Weiss, J. H. Sherman, E. W. McFarland, G. D. Stucky and P. C. Ford, "C1 Coupling via bromine activation and tandem catalytic condensation and neutralization over CaO/Zeolite composites," *Prepr. Pap.-Am. Chem. Soc., Div. Fuel Chem.*, vol. 49, no. 1, pp. 55-56, 2004.
- [27] U. Olsbye, O. V. Saure, N. B. Muddada, S. Bordiga, C. Lamberti, M. H. L. K. P. Nilsen and S. Svelle, "Methane conversion to light olefins-how does the methyl halide route differ from the methanol to olefins (MTO) route?," *Catal. Today*, vol. 171, no. 1, pp. 211-220, 2011.
- [28] Y. Wei, D. Zhang, Z. Liu and B. Su, "Methyl halide to olefins and gasoline over zeolites and SAPO catalysts: a new route of MTO and MTG," *Chin. J. of Catal.*, vol. 33, no. 1, pp. 11-21, 2012.
- [29] E. McFarland, Interviewee, *Methane utilization using halogens*. [Interview]. 25 June 2016.
- [30] E. Gorin, C. Fontana and G. Kidder, "Chlorination of methane with copper chloride melts," *Ind. Eng. Chem.*, vol. 40, no. 11, pp. 2128-2134, 1948.
- [31] A. Baranzini, J. Goldemberg and S. Speck, "A future for carbon taxes," *Ecological Economics*,

vol. 32, no. 3, pp. 395-412, 2000.

- [32] C. Fontana, E. Gorin, G. Kidder and C. Meredith, "Chlorination of methane with copper chloride melts," *Ind. Eng. Chem.*, vol. 44, no. 2, pp. 369-373, 1952.
- [33] J. P. Miller and M. Kling, "Conversion of methane to methanol". United States of America Patent 5243098, 1993.
- [34] P. Grosso, "Zone reactor". United States of America Patent 7361794 B2, 2008.
- [35] W. L. Borkowski, P. E. Oberdorfer and W. H. Seitzer, "Preparation of oxygenated methane derivatives". United States of America Patent 3172915, 1965.
- [36] V. Degirmenci, D. Under and A. Yilmaz, "Methane to Higher Hydrocarbons via Halogenation," *Catal. Today*, vol. 106, no. 1-4, pp. 252-255, 2005.
- [37] S. Gadewar, S. Amin Sadar, P. Grosso, A. Zhang, V. Julka and P. Stolmanov, "Continuous process for converting natural gas to liquid hydrocarbons". United States of America Patent 8921625 B2, 2014.
- [38] I. M. Lorkovic, S. Sun, S. Gadewar, A. Breed, G. S. Macala, A. Sadar, S. E. Cross, J. H. Sherman, G. D. Stucky and P. C. Ford, "Alkane Bromination Revisited: "Reproportionation" in gas-phase methane bromination leads to higher selectivity for CH<sub>3</sub>Br at moderate temperatures," *The J. of Phys. Chem.*, vol. 110, no. 28, pp. 8695-8700, 2006.
- [39] K. Knoche, H. Cremer, D. Breywisch, S. Hegels, G. Steinborn and G. Wuster, "Experimental and theoretical investigation of thermochemical production," *Int. J. Hydrogen Energy*, vol. 3, no. 2, pp. 209-216, 1978.
- [40] D. Van Velzen and H. Langenkamp, "Development studies on the thermochemical cycles for hydrogen production," *Int. J. Hydrogen Energy*, vol. 2, no. 2, pp. 107-121, 1977.
- [41] C. Canavesio, H. E. Nassini and A. E. Bohe, "Evaluation of an iron-chlorine thermochemical cycle for hydrogen production," *Int. J. Hydrogen Energy*, vol. 40, no. 28, pp. 8620-8632, 2015.

- [42] A. K. Manohar, K. Min Kim, E. Plichta, M. Hendrickson, S. Rawlings and S. Narayana, "A high efficiency iron-chloride redox flow battery for large-scale energy storage," *J. Electrochem. Soc.*, vol. 163, no. 1, pp. 5118-5125, 2016.
- [43] M. Bartolozzi, "Development of redox flow batteries. A historical bibliography," *J. Power Sources*, vol. 27, no. 3, pp. 219-234, 1989.
- [44] R. M. Sari, "General Process Plant Cost Estimating (Engineering Design Guideline)," KLM Technology Group, 2014.
- [45] R. Sinnott, *Chemical Engineering Design*, 5th Edition, Butterworth-Heinemann, 2009.
- [46] Environmental Protection Agency, *Carbon Pollution Emission Guidelines for Existing Stationary Sources: Electric Utility Generating Units; Final Rule*, National Archives and Records Administration, 2015.
- [47] AspenTech, "Aspen Physical Property System: Physical Property Methods," Burlington, 2011.
- [48] H. Johnstone and H. W. W. E. Weingartner, "The System Ferric Chloride-Sodium Chloride," *J. Am. Chem. Soc.*, vol. 64, no. 2, pp. 241-244, 1942.
- [49] D. S. Rustad and N. W. Gregory, "Vapor Pressure of Iron(III) Chloride," *J. Chem. Eng. Data*, vol. 28, no. 2, pp. 151-155, 1983.
- [50] V. Julka, S. Gadewar, P. Stoimenov, P. Grosso, J. Sherman and A. Zhang, "Conversion of Propane to Propylene". United States of America Patent 8940954, 27 January 2015.
- [51] E. Sada, S. Katoh, H. Yoshil, T. Yamanishi and A. Nakanishi, "Performance of the Gas Bubble Column in Molten Salt Systems," *Ind. Eng. Chem. Process Des. Dev.*, vol. 23, no. 1, pp. 151-154, 1984.
- [52] H. M. Pitt and B. Harry, "Production of Chloroform". United States of America Patent 3026361 A, 1962.
- [53] R. P. Tomkins and N. P. Bansal, *Gases in Molten Salts*, vol. 45/46, New Jersey: Pergamon Press,

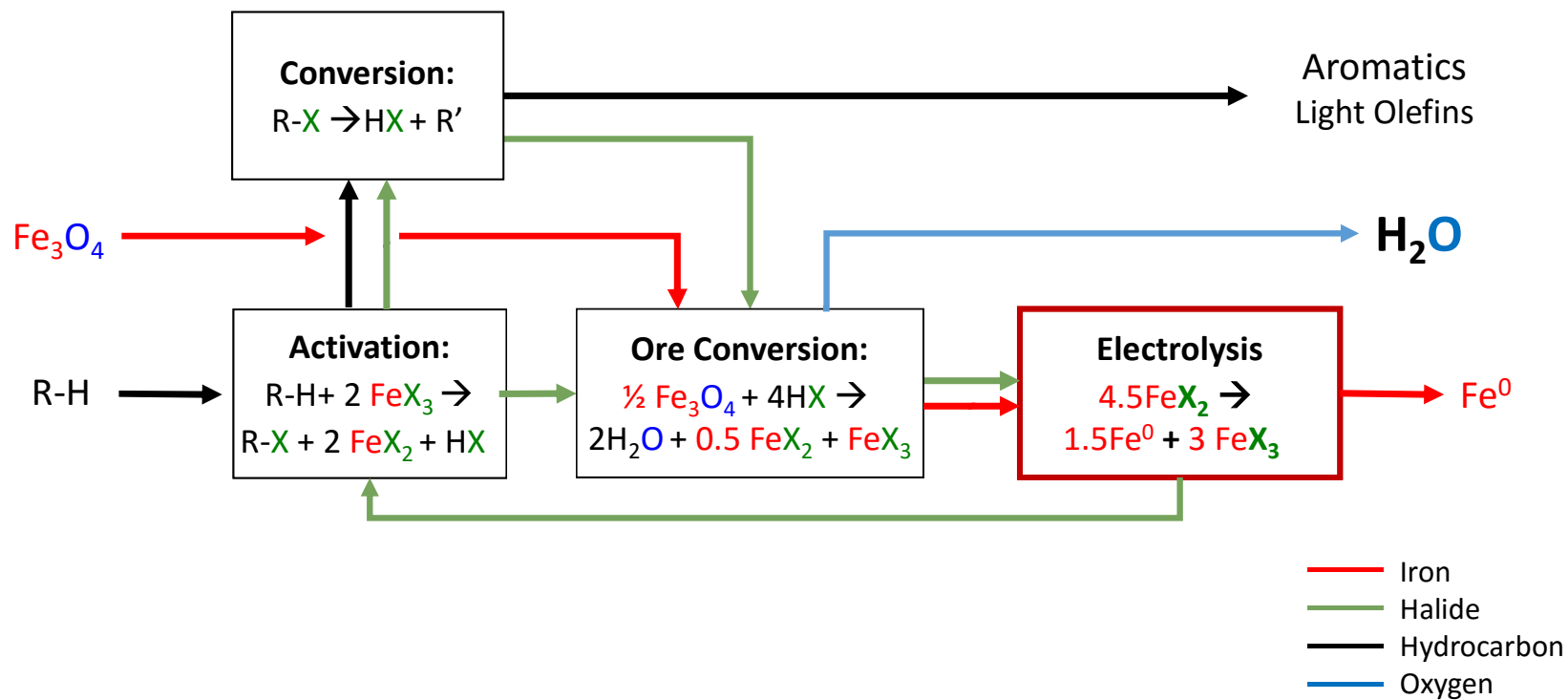
1991.

- [54] H. G. Hamilton and D. Inman, "Solubility of Hydrogen Chloride in Zinc Chloride," *J. Chem. Eng. Data*, vol. 37, no. 4, pp. 456-458, 1992.
- [55] Y. Tadokoro, T. Kajiyama, T. Yamaguchi, N. Sakai, H. Kameyama and K. Yoshidas, "Technical evaluation of UT-3 Thermochemical hydrogen production process for an industrial scale plant," *Int. J. Hydrogen Energy*, vol. 22, no. 1, pp. 49-56, 1997.
- [56] R. Salmimies, "Acidic dissolution of iron oxides and regeneration of a ceramic filter medium," Lappeenranta University of Technology, Lappeenranta, 2012.
- [57] L. Hruska and R. Savinell, "Investigation of Factors Affecting Performance of the Iron-Redox Battery," *J. Electrochem. Soc.*, vol. 128, no. 1, pp. 18-25, 1981.
- [58] M. A. Miller, J. Wainright and R. Savinell, "Communication - Iron Ionic Liquid Electrolytes for Redox Flow Battery Applications," *J. Electrochem. Soc.*, vol. 163, no. 3, pp. 578-579, 2016.
- [59] H. Lang, "Cost relationships in preliminary cost estimation," *Chem. Eng.*, vol. 54, pp. 117-121, 1947.
- [60] Steel on the Net, "Steelmaking Commodity Prices," Steel on the Net, 1st July 2016. [Online]. Available: <http://www.steelonthenet.com/commodity-prices.html>. [Accessed July 2016].
- [61] ICIS, "Indicative Chemical Prices A-Z," ICIS, 2007. [Online]. Available: <http://www.icis.com/chemicals/channel-info-chemicals-a-z/>. [Accessed July 2016].
- [62] M. Pyziur, "Condensate; An EPRINC Primer," Energy Policy Research Foundation, Washington, 2015.
- [63] EIA, "Annual Energy Outlook 2016," EIA, July 2016. [Online]. Available: [https://www.eia.gov/forecasts/aeo/executive\\_summary.cfm](https://www.eia.gov/forecasts/aeo/executive_summary.cfm). [Accessed July 2016].
- [64] EIA, "U.S. Energy Information Administration," EIA, 26 July 2016. [Online]. Available: [https://www.eia.gov/electricity/monthly/epm\\_table\\_grapher.cfm?t=epmt\\_5\\_6\\_a](https://www.eia.gov/electricity/monthly/epm_table_grapher.cfm?t=epmt_5_6_a). [Accessed

July 2016].

ACCEPTED MANUSCRIPT





**Highlights**

- A CO<sub>2</sub>-free integrated iron and hydrocarbon process utilizing molten salt electrolysis is proposed
- Partial oxidation of natural gas alkanes using a liquid metal halide (FeCl<sub>3</sub>) as the oxidising agent
- Generates a high-value electrolysis feedstock through leaching the iron ore with inorganic acids
- Metallic halide feedstock is regenerated through the coproduction of reduced iron
- Process economics are competitive with low imposed carbon prices

ACCEPTED MANUSCRIPT